Letter

Three-loop helicity amplitudes for photon+jet production

Piotr Bargiela,[1,*] Amlan Chakraborty,[2,†] and Giulio Gambuti[1,‡]
[1]*Rudolf Peierls Centre for Theoretical Physics, University of Oxford, Clarendon Laboratory, Parks Road, Oxford OX1 3PU, United Kingdom*
[2]*University at Buffalo, The State University of New York, Buffalo 14260, USA*

(Received 17 January 2023; accepted 10 February 2023; published 14 March 2023)

We present three-loop helicity amplitudes for the production of a single photon in association with one jet in quantum chromodynamics, a final state which provides a standard candle of the Standard Model at the Large Hadron Collider. We employ a recently proposed variation of the so-called tensor projection method in the 't Hooft-Veltman scheme (tHV) which avoids the computation of contributions due to unphysical (-2ϵ)-dimensional polarizations of the external states. We obtain compact analytic results expressed in terms of harmonic polylogarithms.

DOI: 10.1103/PhysRevD.107.L051502

I. INTRODUCTION

Scattering amplitudes are one of the central quantities in quantum field theory. In addition to the intrinsic beauty of their mathematical structure, they provide a bridge between theory and experiment. High-precision amplitudes in quantum chromodynamics (QCD) are essential to compute accurate theoretical predictions that, together with increasingly precise measurements from colliders, allows for a scrutiny of the structure of the Standard Model, and for constraining new physics models.

It is well known that the number of external particles and of internal loops greatly influences the complexity of amplitude calculations. Up until a few years ago, the state of the art for massless four-particle scattering was the three-loop four-gluon amplitude in $\mathcal{N}=4$ super-Yang-Mills [1], where calculations are simplified by the high amount of symmetry in the theory. The same amplitude was also computed in the planar limit of pure Yang-Mills in Ref. [2]. In QCD similar three-loop calculations proved until recently to be too computationally prohibitive to be performed due to the lack of symmetry.

The first analytic results for a QCD three-loop four-point amplitude were obtained for the color singlet process $q\bar{q} \to \gamma\gamma$ in Ref. [3]. Building on this, the more computationally involved color singlet production $gg \to \gamma\gamma$ was computed in Ref. [4]. Finally, all amplitudes involving four colored partons, i.e., $gg \to gg$, $q\bar{q} \to q\bar{q}$, $q\bar{q} \to gg$ and all possible crossings of external states, were obtained in Refs. [5–7]. In these processes, starting a three loops, there start appearing new contributions to the structure of infrared (IR) divergences. These are associated with the exchange of color charge between all four external legs through the emission and absorption of soft gluons. This is referred to as *quadrupole radiation* and it increases the complexity of the corresponding amplitudes.

In this work we tackle the last three-loop four-point massless amplitudes in QCD involving partonic initial states: $gg \to g\gamma$ and $q\bar{q} \to g\gamma$.

Phenomenologically, this amplitude is relevant for the $pp \to \gamma + j$ process, i.e., direct photon production with a reconstructed jet. It is one of the standard candles of the Standard Model at the Large Hadron Collider (LHC). Theoretical QCD predictions for this process exist at the next-to-next-to-leading order (NNLO) [8]. Providing even higher order corrections would lead to a more precise comparison with the LHC data, which is important for current and especially future LHC runs [8]. The three-loop amplitudes in quark-pair and quark+gluon initiated channels contribute to the N3LO cross section. The three-loop gluon-pair initiated amplitude starts contributing only at N4LO, however it is enhanced by the parton distribution function (PDF) of the gluon, which may at least partially compensate for the strong coupling suppression.

For photon+jet production at hadron colliders, we consider the two independent partonic channels

$$\begin{aligned} &g(p_1) + g(p_2) \to g(-p_3) + \gamma(-p_4), \\ &q(p_1) + \bar{q}(p_2) \to g(-p_3) + \gamma(-p_4). \end{aligned} \tag{1}$$

*piotr.bargiela@physics.ox.ac.uk
†amlancha@buffalo.edu
‡giulio.gambuti@physics.ox.ac.uk

The remaining $qg \to q\gamma$ and $\bar{q}g \to \bar{q}\gamma$ channels can be obtained via crossing of $q\bar{q} \to g\gamma$. We treat all four-momenta as incoming and massless

$$p_1 + p_2 + p_3 + p_4 = 0, \qquad p_i^2 = 0. \tag{2}$$

The kinematic Mandelstam invariants of the process,

$$s = (p_1 + p_2)^2, \quad t = (p_1 + p_3)^2, \quad u = (p_2 + p_3)^2, \tag{3}$$

are related by momentum conservation $s + t + u = 0$. Since the overall mass dimension of the amplitude is fixed, the non-trivial kinematic dependence can be expressed in terms of a single dimensionless ratio

$$x = -\frac{t}{s}. \tag{4}$$

On the physical Riemann sheet, we have[1]

$$s > 0, t < 0, u < 0, \qquad s_{ij} \to s_{ij} + i\delta, \tag{5}$$

where $s_{ij} = 2p_i \cdot p_j$.

This paper is organized as follows: in Sec. II we describe the color and Lorentz space decomposition of the amplitudes. The definition of the helicity amplitudes is given in Sec. III where we also fix our notation within the spinor helicity formalism and describe the workflow used for this computation. Section IV describes renormalization and IR subtraction of the helicity amplitudes. Finally, we give more details on the results in Sec. V and provide concluding remarks in Sec. VI.

II. COLOR AND TENSOR STRUCTURES

For both processes in Eq. (1) we can collect an overall color factor $\mathcal{C}$ in front of the amplitude:

$$\mathcal{A} = \mathcal{C}A, \tag{6}$$

where

$$\mathcal{C} = \begin{cases} \mathrm{Tr}(T^{a_1}T^{a_2}T^{a_3}) - (2 \leftrightarrow 3), & \text{for } gg \to g\gamma, \\ T^{a_3}_{i_1 i_2}, & \text{for } q\bar{q} \to g\gamma. \end{cases} \tag{7}$$

Above $i_n(a_n)$ refers to a $SU(N_c)$ index in the fundamental (adjoint) representation and T^a are the fundamental generators of $SU(N_c)$, normalized such that $\mathrm{Tr}(T^a T^b) = \frac{1}{2}\delta^{ab}$. The color stripped amplitude A depends on the number of active quark flavors n_f, the electric coupling of the different quark flavors Q_f and the fermionic loop factor

$$n_f^{(V)} = \sum_{f=1}^{n_f} Q_f. \tag{8}$$

After extracting all color structures, A can be further decomposed onto a basis of n_t independent Lorentz tensor structures

$$A = \sum_{i=1}^{n_t} T_i \mathcal{F}_i. \tag{9}$$

We work in the 't Hooft-Veltman (tHV) regularization scheme, where internal states are in d dimensions but the external momenta and polarizations are kept in 4 dimensions. In this scheme, we follow a recent proposal [9,10] that allows us to remove the irrelevant (-2ϵ)-dimensional external helicity states and to work with a set of tensors T_i whose number coincides with that of the independent helicity configurations. In the $gg \to g\gamma$ channel, $n_t = 8$ and with the cyclic gauge $\epsilon_i \cdot p_{i+1} = 0$ and $p_5 \equiv p_1$ we find

$$\begin{aligned} T_1 &= p_1 \cdot \epsilon_2 p_1 \cdot \epsilon_3 p_2 \cdot \epsilon_4 p_3 \cdot \epsilon_1, \\ T_2 &= \epsilon_3 \cdot \epsilon_4 p_1 \cdot \epsilon_2 p_3 \cdot \epsilon_1, \qquad T_3 = \epsilon_2 \cdot \epsilon_4 p_1 \cdot \epsilon_3 p_3 \cdot \epsilon_1, \\ T_4 &= \epsilon_2 \cdot \epsilon_3 p_2 \cdot \epsilon_4 p_3 \cdot \epsilon_1, \qquad T_5 = \epsilon_1 \cdot \epsilon_4 p_1 \cdot \epsilon_2 p_1 \cdot \epsilon_3, \\ T_6 &= \epsilon_1 \cdot \epsilon_3 p_1 \cdot \epsilon_2 p_2 \cdot \epsilon_4, \qquad T_7 = \epsilon_1 \cdot \epsilon_2 p_1 \cdot \epsilon_3 p_2 \cdot \epsilon_4, \\ T_8 &= \epsilon_1 \cdot \epsilon_2 \epsilon_3 \cdot \epsilon_4 + \epsilon_1 \cdot \epsilon_4 \epsilon_2 \cdot \epsilon_3 + \epsilon_1 \cdot \epsilon_3 \epsilon_2 \cdot \epsilon_4. \end{aligned} \tag{10}$$

In the $q\bar{q} \to g\gamma$ channel, $n_t = 4$ and with the gauge choice $\epsilon_3 \cdot p_2 = \epsilon_4 \cdot p_1 = 0$ we get

$$\begin{aligned} T_1 &= \bar{u}(p_2) \not{\epsilon}_3 u(p_1) \epsilon_4 \cdot p_2, \\ T_2 &= \bar{u}(p_2) \not{\epsilon}_3 u(p_1) \epsilon_4 \cdot p_1, \\ T_3 &= \bar{u}(p_2) \not{p}_3 u(p_1) \epsilon_3 \cdot p_1 \epsilon_4 \cdot p_2, \\ T_4 &= \bar{u}(p_2) \not{p}_3 u(p_1) \epsilon_3 \cdot \epsilon_4. \end{aligned} \tag{11}$$

The form factors $\mathcal{F}_i$ can be extracted from A with appropriate projectors P_j, defined such that $\sum_{\mathrm{pol}} P_j T_i = \delta_{ji}$, see e.g. Refs. [9,10] for the full discussion.

III. HELICITY AMPLITUDES

In order to obtain the helicity amplitudes $A_{\vec{\lambda}}$, it is enough to evaluate the tensors T_i for fixed-helicity configurations $\vec{\lambda}$. This is equivalent to a simple change of basis, and the helicity amplitude for the helicity configuration $\vec{\lambda} = \{\lambda_1, \lambda_2, \lambda_3, \lambda_4\}$ can be written as a linear combination of form factors $\mathcal{F}_i$

$$A_{\vec{\lambda}} = \sum_{i=1}^{n_t} T_{i,\vec{\lambda}} \mathcal{F}_i = \mathcal{S}_{\vec{\lambda}} \mathcal{H}_{\vec{\lambda}}. \tag{12}$$

[1]Technically, Eq. (5) is imprecise since the condition $s + t + u = 0$ has to be always satisfied. This makes analytic continuation for massless $2 \to 2$ scattering delicate, see e.g. Ref. [6] for a discussion in the context of three-loop amplitudes.

The overall spinor factors $\mathcal{S}_{\vec{\lambda}}$ can be extracted from $A_{\vec{\lambda}}$ using the spinor-helicity formalism, see e.g. Ref. [11] for a pedagogical introduction. In this notation, fixed-helicity external quarks are defined as

$$|p\rangle = \overline{[p|} = \frac{1+\gamma_5}{2}u(p), \quad |p] = \overline{\langle p|} = \frac{1-\gamma_5}{2}u(p), \tag{13}$$

with $[p| = \bar{u}(p)\frac{1-\gamma_5}{2}$ and $\langle p| = u(p)\frac{1+\gamma_5}{2}$ treating particles and antiparticles on the same footing, while polarization vectors take the following form

$$\epsilon^{\mu}_{j,+}(p_j) = \frac{\langle p_j|\gamma^{\mu}|q_j]}{\sqrt{2}[p_j q_j]}, \qquad \epsilon^{\mu}_{j,-}(p_j) = \frac{\langle q_j|\gamma^{\mu}|p_j]}{\sqrt{2}\langle q_j p_j\rangle}, \tag{14}$$

where q_i is the massless reference vector corresponding to the ith external gluon and is chosen consistently with the gauge conditions used to determine the tensor bases of Eqs. (10) and (11). For the $gg \to g\gamma$ channel we have $q_i = p_{i+1}$, where we identify $p_5 \equiv p_1$ and we choose the spinor factors to be

$$\begin{aligned}
\mathcal{S}_{++++} &= \frac{\langle 12\rangle\langle 34\rangle}{[12][34]}, & \mathcal{S}_{-+++} &= \frac{[12][14]\langle 24\rangle}{[34][23][24]},\\
\mathcal{S}_{+-++} &= \frac{[21][24]\langle 14\rangle}{[34][13][14]}, & \mathcal{S}_{++-+} &= \frac{[32][34]\langle 24\rangle}{[14][21][24]},\\
\mathcal{S}_{+++-} &= \frac{[42][43]\langle 23\rangle}{[13][21][23]}, & \mathcal{S}_{--++} &= \frac{[12]\langle 34\rangle}{\langle 12\rangle[34]},\\
\mathcal{S}_{-+-+} &= \frac{[13]\langle 24\rangle}{\langle 13\rangle[24]}, & \mathcal{S}_{+--+} &= \frac{[23]\langle 14\rangle}{\langle 23\rangle[14]},
\end{aligned} \tag{15}$$

while for the $q\bar{q} \to g\gamma$ channel we have $q_3 = p_2$, $q_4 = p_1$ and define the spinor factors as

$$\begin{aligned}
\mathcal{S}_{-+--} &= \frac{2[34]^2}{\langle 13\rangle[23]}, & \mathcal{S}_{-+-+} &= \frac{2\langle 24\rangle[13]}{\langle 23\rangle[24]},\\
\mathcal{S}_{-++-} &= \frac{2\langle 23\rangle[41]}{\langle 24\rangle[32]}, & \mathcal{S}_{-+++} &= \frac{2\langle 34\rangle^2}{\langle 31\rangle[23]}.
\end{aligned} \tag{16}$$

The spinor-free helicity amplitude $\mathcal{H}_{\vec{\lambda}}$ can be expanded as a QCD perturbative series

$$\mathcal{H}_{\vec{\lambda}} = \sqrt{4\pi\alpha}\sqrt{4\pi\alpha_{s,b}}\sum_{\ell=0}^{3}\left(\frac{\alpha_{s,b}}{4\pi}\right)^{\ell}\mathcal{H}^{(\ell)}_{\vec{\lambda}}, \tag{17}$$

where we have factored out an overall electric coupling $e = \sqrt{4\pi\alpha}$ as well as a bare strong coupling $g_{s,b} = \sqrt{4\pi\alpha_{s,b}}$. $\mathcal{H}^{(\ell)}_{\vec{\lambda}}$ corresponds to the bare ℓ-loop amplitude. Note that since the $gg \to g\gamma$ channel is loop-induced, the first term in its perturbative expansion vanishes. Conversely, the $q\bar{q} \to g\gamma$ channel contributes nontrivially at all four orders. The main objective of this paper is to compute the three-loop term $\mathcal{H}^{(3)}_{\vec{\lambda}}$. As a by-product of our work, we have also recomputed all lower-loop amplitudes. We checked all one-loop helicity amplitudes numerically against OPENLOOPS [12,13]. At the two-loop level, to the best of our knowledge, the only available analytic results are for the process $q\bar{q} \to g\gamma$ and are given in Ref. [14] in the form of a color- and polarization-summed interference with the tree-level, with which we found perfect agreement.[2] We generate Feynman diagrams corresponding to each channel with QGRAF [16] (see sample diagrams in Fig. 1). At three loops, there are 7356 graphs in the $gg \to g\gamma$ channel, and 5534 graphs in the $q\bar{q} \to g\gamma$ channel. Then, we perform color and Dirac algebra using FORM [17]. There are $\mathcal{O}(10^6)$ scalar Feynman integrals contributing to the form factors of each of the scattering process described in Eq. (1). Since the integrals at hand are not all linearly independent, we can find relations between them. Preliminarily, we exploited loop-momentum shift-invariance to reduce the complexity by a factor of about 20. This is then followed by the most complicated step, which involves integration-by-parts (IBP) identities [18] to relate the remaining integrals to a minimal independent basis set of master integrals (MIs). In order to perform the IBP reduction, we have used the Laporta algorithm [19] implemented in REDUZE 2 [20,21], as well as in FINRED [22], which exploits syzygy-based techniques [23–28] and finite-field arithmetic [22,29–31]. In this manner, we are left with 486 independent MIs. They have been computed analytically as a series in the

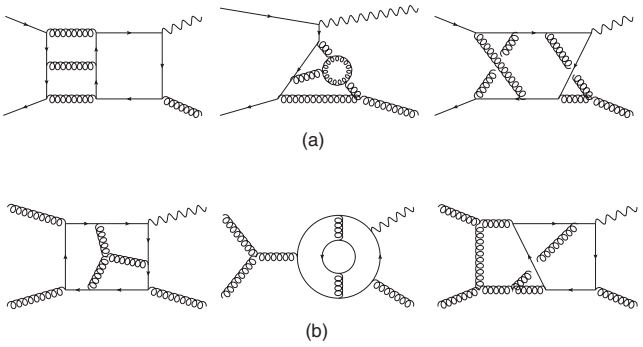

FIG. 1. Sample three-loop diagrams for (a) the process $q\bar{q} \to g\gamma$ and (b) the process $gg \to g\gamma$.

[2]The results presented in Ref. [14] are computed in the conventional dimensional regularization (CDR) scheme and with a IR subtraction scheme which differs from the one adopted in this paper. While the difference in dimensional regularization scheme is immaterial at the level of the $O(\epsilon^0)$ part of the finite remainder provided by the authors of Ref. [14], the difference in IR subtraction scheme is not. In order to bridge the gap, we performed a second subtraction of the IR poles of our two loop renormalized amplitudes using the definition of the finite part in Ref. [15], and combined all helicity amplitudes to obtain the same quantity computed in Ref. [14].

dimensional regulator $\epsilon = (4-d)/2$ in terms of harmonic polylogarithms (HPLs) [32] in Ref. [33] and later in Ref. [4]. The evaluation of MIs is based on the differential equation approach applied to a canonical basis of master integrals [34]. Substituting expressions for MIs leads to the final formula for the bare three-loop amplitude, expanded to $\mathcal{O}(\epsilon^0)$ with HPLs up to transcendental weight 6.

IV. UV RENORMALIZATION AND IR REGULARIZATION

The divergences appearing in the amplitudes treated in this paper are both of ultraviolet (UV) and infrared (IR) origin. When working in dimensional regularization they are represented by poles in the dimensional regulator ϵ. By defining the $\overline{\text{MS}}$ renormalized strong coupling $\alpha_s(\mu)$ through the equation

$$\bar{\alpha}_{s,b}\mu_0^{2\epsilon} S_\epsilon = \bar{\alpha}_s(\mu)\mu^{2\epsilon} Z[\bar{\alpha}_s(\mu)], \tag{18}$$

one can obtain UV-finite amplitudes. Above, we have defined for convenience $\bar{\alpha}_{s,b} = \alpha_{s,b}/(4\pi)$ and $\bar{\alpha}_s(\mu) = \alpha_s(\mu)/(4\pi)$. The quantity μ is the renormalization scale introduced in dimensional regularization and $Z[\bar{\alpha}_s]$ reads

$$\begin{aligned} Z[\bar{\alpha}_s] = 1 &- \bar{\alpha}_s \frac{\beta_0}{\epsilon} + \bar{\alpha}_s^2 \left(\frac{\beta_0^2}{\epsilon^2} - \frac{\beta_1}{2\epsilon}\right) \\ &- \bar{\alpha}_s^3 \left(\frac{\beta_0^3}{\epsilon^3} - \frac{7}{6}\frac{\beta_0\beta_1}{\epsilon^2} + \frac{\beta_2}{3\epsilon}\right) + \mathcal{O}(\bar{\alpha}_s^4). \end{aligned} \tag{19}$$

The explicit form of the β-function coefficients β_i can be found in Supplemental Material [35]. The perturbative contributions to the UV-renormalized helicity amplitudes $\mathcal{H}_{\vec{\lambda},\text{ren}}$ are obtained by expanding Eq. (17) in $\bar{\alpha}_s(\mu)$.

The poles in ϵ appearing in the renormalized amplitudes are of IR nature and their structure was described at two loops in [15] and generalized to different processes [36–38] and to three loops in Refs. [39–44]. They assume a universal form across all massless gauge theories. Up to the three loop-order, one can write [39,40]

$$\mathcal{H}_{\vec{\lambda},\text{ren}} = \mathcal{Z}_{\text{IR}} \mathcal{H}_{\vec{\lambda},\text{fin}}, \tag{20}$$

where $\mathcal{H}_{\vec{\lambda},\text{fin}}$ are *finite remainders* and $\mathcal{Z}_{\mathcal{IR}}$ is in general a color operator that acts on the color structure of the amplitudes. It can be written in terms of the so-called soft anomalous dimension $\mathbf{\Gamma}$ as

$$\mathcal{Z}_{\text{IR}} = \mathbb{P}\exp\left[\int_\mu^\infty \frac{\mathrm{d}\mu'}{\mu'} \mathbf{\Gamma}(\{p\},\mu')\right], \tag{21}$$

where the *path ordering* operator $\mathbb{P}$ reorganises color operators in increasing values of μ' from left to right and is immaterial up to three loops since to this order $[\mathbf{\Gamma}(\mu), \mathbf{\Gamma}(\mu')] = 0$. The soft anomalous dimension can be written as

$$\mathbf{\Gamma} = \mathbf{\Gamma}_{\text{dip}} + \mathbf{\Delta}_4. \tag{22}$$

The *dipole* term $\mathbf{\Gamma}_{\text{dip}}$ is due to the pairwise exchange of color charge between external legs and reads

$$\mathbf{\Gamma}_{\text{dip}} = \sum_{1\le i<j\le 4} \mathbf{T}_i^a \mathbf{T}_j^a \gamma^{\text{K}} \ln\left(\frac{\mu^2}{-s_{ij} - i\delta}\right) + \sum_{i=1}^4 \gamma^i, \tag{23}$$

where $s_{ij} = 2p_i \cdot p_j$, γ^{K} is the *cusp anomalous dimension* [45–52] and $\gamma^{i=q,g}$ are the *quark and gluon anomalous dimensions* [53–56]. In Eq. (23) we have also introduced the standard color insertion operators $\mathbf{T}_i^a$, which only act on the ith external color index. Their action on the color factors of our amplitudes is defined as follows:

$$\begin{aligned} (\mathbf{T}_i^a)_{b_i c_i} &= -i f^a{}_{b_i c_i} \quad \text{for a gluon,} \\ (\mathbf{T}_i^a)_{i_i j_i} &= +T^a_{i_i j_i} \quad \text{for a (initial)final state (anti)quark,} \\ (\mathbf{T}_i^a)_{i_i j_i} &= -T^a_{j_i i_i} \quad \text{for a (final)initial state (anti)quark,} \\ \mathbf{T}_i^a &= 0 \quad \text{for a photon.} \end{aligned} \tag{24}$$

Performing the color algebra with the definitions in Eq. (24) we find the explicit value of the dipole anomalous dimensions in the two channels under consideration. Note that, since the amplitudes considered here feature a single color structure, $\mathbf{\Gamma}$ acts by simple scalar multiplication. For $q\bar{q} \to g\gamma$ it reads

$$\begin{aligned} \mathbf{\Gamma}_{\text{dip}}^{q\bar{q}\to g\gamma} = \frac{1}{2}\Bigg\{ &\frac{1}{N_c}\ln\left(\frac{\mu^2}{-s-i\delta}\right) \\ &+ -N_c\left[\ln\left(\frac{\mu^2}{-t-i\delta}\right) + \ln\left(\frac{\mu^2}{-u-i\delta}\right)\right]\Bigg\}\gamma^{\text{K}} \\ &+ 2\gamma^q + \gamma^g, \end{aligned} \tag{25}$$

while for $gg \to g\gamma$ we get

$$\begin{aligned} \mathbf{\Gamma}_{\text{dip}}^{gg\to g\gamma} = -\frac{N_c}{2}\Bigg\{ &\ln\left(\frac{\mu^2}{-s-i\delta}\right) + \ln\left(\frac{\mu^2}{-t-i\delta}\right) \\ &+ \ln\left(\frac{\mu^2}{-u-i\delta}\right)\Bigg\}\gamma^{\text{K}} + 3\gamma^g. \end{aligned} \tag{26}$$

The *quadrupole* contribution $\mathbf{\Delta}_4$ in Eq. (22) accounts instead for the exchange of color charge among (up to) four external legs and it appears for the first time at three loops, $\mathbf{\Delta}_4 = \sum_{n=3}^\infty \bar{\alpha}_s^n \mathbf{\Delta}_4^{(n)}$. Because the amplitudes considered in this paper feature only three colored external states, $\mathbf{\Delta}_4$ assumes a simpler form compared to the full result given in Ref. [44]. In addition to this, the perturbative series for

$gg \to g\gamma$ starts at one loop and therefore it receives no quadrupole correction at three loops.

For $q\bar{q} \to g\gamma$, the relevant contribution reads

$$\mathbf{\Delta}_4^{(3),q\bar{q}\to g\gamma} = -24N_c(\zeta_5 + 2\zeta_2\zeta_3). \tag{27}$$

We verified that the IR singularities of our three-loop amplitudes match perfectly those generated by Eqs. (20)–(27), which provides a highly non-trivial check of our results.

V. RESULTS

The expressions we obtained for the finite remainder $\mathcal{H}^{(\ell)}_{\vec{\lambda},\text{fin}}$ are relatively compact, but still too long to be included in this manuscript. They are provided in computer-readable format in the Supplemental Material [35].

We also provide the explicit results for the channel $qg \to q\gamma$ which can be generated by crossing the $q\bar{q} \to g\gamma$ amplitude. The only other relevant channel for $pp \to j\gamma$ is $\bar{q}g \to \bar{q}\gamma$ and it can be obtained by charge conjugation of $qg \to q\gamma$, which leaves the helicity-stripped amplitudes unchanged. When crossing the amplitudes, one has to permute Mandelstam invariants. In doing so, it is important not to cross more then one branch cut per transformation. This can be guaranteed by an appropriate composition of multiple transformations. All needed manipulations of HPLs can be performed with POLYLOGTOOLS [57], and the procedure is described in more detail in Ref. [6]. It is also worth pointing out that when applying a crossing or a charge/parity transformation to the amplitudes associated to the processes in Eq. (1), one has to take care of applying the corresponding transformations to the spinor weights in Eqs. (15) and (16).

Finally, we point out that our amplitudes can be evaluated numerically in an efficient way since they consist of only rational, and well-studied HPL functions. In Fig. 2 we provide sample plots for the $q\bar{q} \to g\gamma$ and $gg \to g\gamma$ channels, where we numerically evaluated the squared amplitudes normalized to the leading order. To define the quantities plotted in the figure more precisely, we first introduce the notation

$$\langle \mathcal{A}^{(\ell)} | \mathcal{A}^{(\ell')} \rangle \equiv \sum_{f,\vec{\lambda},\text{col}} \mathcal{C}^\dagger \mathcal{C} |s_{\vec{\lambda}}|^2 \mathcal{H}^{(\ell)^*}_{\vec{\lambda},\text{fin}} \mathcal{H}^{(\ell')}_{\vec{\lambda},\text{fin}} \tag{28}$$

for the interference between two amplitudes summed over all internal quark flavors, all helicity configurations and all colors of the external states. With this, we can write

$$\begin{aligned}
\mathcal{V}^{(\text{NLO})}_{q\bar{q}\to g\gamma} &= \frac{2\text{Re}\langle \mathcal{A}^{(0)} | \mathcal{A}^{(1)} \rangle}{\langle \mathcal{A}^{(0)} | \mathcal{A}^{(0)} \rangle}, \\
\mathcal{V}^{(\text{NNLO})}_{q\bar{q}\to g\gamma} &= \frac{\langle \mathcal{A}^{(1)} | \mathcal{A}^{(1)} \rangle}{\langle \mathcal{A}^{(0)} | \mathcal{A}^{(0)} \rangle} + \frac{2\text{Re}\langle \mathcal{A}^{(0)} | \mathcal{A}^{(2)} \rangle}{\langle \mathcal{A}^{(0)} | \mathcal{A}^{(0)} \rangle}, \\
\mathcal{V}^{(\text{N3LO})}_{q\bar{q}\to g\gamma} &= \frac{2\text{Re}\langle \mathcal{A}^{(1)} | \mathcal{A}^{(2)} \rangle}{\langle \mathcal{A}^{(0)} | \mathcal{A}^{(0)} \rangle} + \frac{2\text{Re}\langle \mathcal{A}^{(0)} | \mathcal{A}^{(3)} \rangle}{\langle \mathcal{A}^{(0)} | \mathcal{A}^{(0)} \rangle},
\end{aligned} \tag{29}$$

and

$$\begin{aligned}
\mathcal{V}^{(\text{N3LO})}_{gg\to g\gamma} &= \frac{2\text{Re}\langle \mathcal{A}^{(1)} | \mathcal{A}^{(2)} \rangle}{\langle \mathcal{A}^{(1)} | \mathcal{A}^{(1)} \rangle}, \\
\mathcal{V}^{(\text{N4LO})}_{gg\to g\gamma} &= \frac{\langle \mathcal{A}^{(2)} | \mathcal{A}^{(2)} \rangle}{\langle \mathcal{A}^{(1)} | \mathcal{A}^{(1)} \rangle} + \frac{2\text{Re}\langle \mathcal{A}^{(1)} | \mathcal{A}^{(3)} \rangle}{\langle \mathcal{A}^{(1)} | \mathcal{A}^{(1)} \rangle},
\end{aligned} \tag{30}$$

where the process dependence has been left implicit. We point out that the quantities plotted in Fig. 2 nicely show convergence of the loop corrections, however it should be kept in mind that they depend on the choice of IR subtraction scheme and only represent the virtual

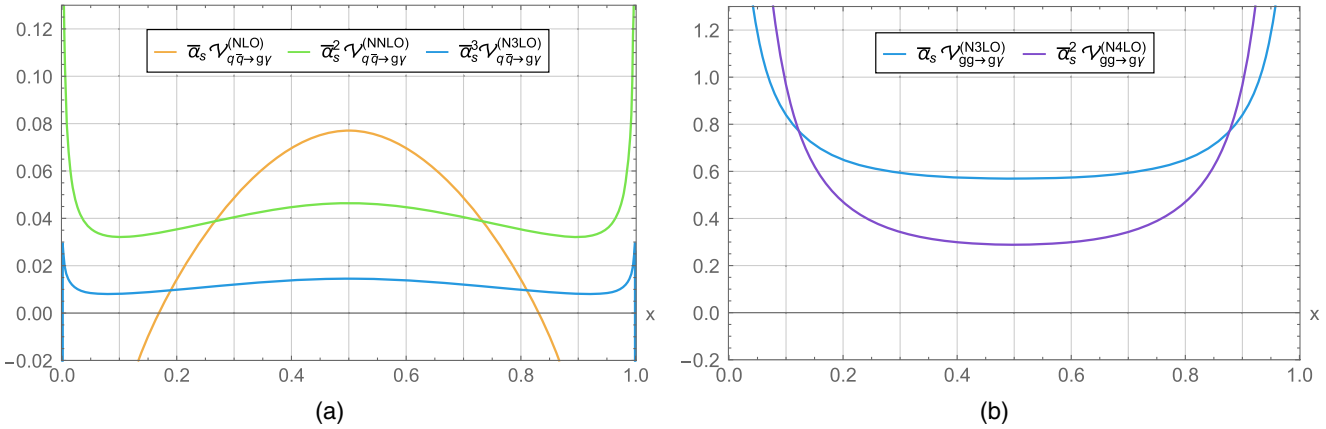

FIG. 2. Perturbative expansions of the color, helicity and flavor summed finite remainder of the amplitude squared for the process (a) $q\bar{q} \to g\gamma$ and (b) $gg \to g\gamma$ as a function of $x = -t/s$ normalized to the corresponding leading order. For simplicity we set $\alpha_s = 0.118$, $\mu^2 = s$, $N_c = 3$, $n_f = 5$ and $n_f^{(V)} = 1/3$. The (NnLO) labels are assigned in terms of the contribution to the process $pp \to g\gamma$.

contributions to the partonic cross section. In addition, for the $q\bar{q} \to g\gamma$ channel we observe the same alternating behavior of the different perturbative orders when approaching the limits $x \to 0$ and $x \to 1$ that is also present in the $q\bar{q} \to gg$ and $gg \to gg$ channels [7].

VI. CONCLUSIONS

In this paper we have completed the computation of the last three-loop four-point massless QCD scattering amplitudes with partons in the initial state. To do so, we employed a refined version of the tensor projection method which considerably reduces the amount of calculations required. At one and two loops, we have checked the consistency of our result against the available literature and found perfect agreement. At three loops, our amplitudes have the correct UV and IR structure, including the quadrupole contribution that appears at this perturbative order for the first time. The corrections provided in this paper start contributing to the differential cross section at N3LO and in the future they will hopefully allow to achieve better precision on the prediction of photon+jet observables at hadron colliders.

ACKNOWLEDGMENTS

We are grateful to A. von Manteuffel for providing the IBP relations through his private code FINRED. We also thank F. Caola and L. Tancredi for insightful discussions and comments on this manuscript. A. C. is grateful to the Department of Physics and Astronomy, Michigan State University for the hospitality for the time during which the initial part of the calculation was performed. The research of P. B. was supported by the ERC Starting Grant No. 804394 HipQCD. A. C. was supported by the National Science Foundation by Grants No. PHY-1652066 and No. NSF-PHY-2014021. G. G. was supported by the Royal Society Grant No. URF/R1/191125.

[1] J. M. Henn and B. Mistlberger, Four-Gluon Scattering at Three Loops, Infrared Structure, and the Regge Limit, Phys. Rev. Lett. **117**, 171601 (2016).
[2] Q. Jin and H. Luo, Analytic form of the three-loop four-gluon scattering amplitudes in Yang-Mills theory, arXiv:1910.05889.
[3] F. Caola, K. Melnikov, D. Napoletano, and L. Tancredi, Noncancellation of infrared singularities in collisions of massive quarks, Phys. Rev. D **103**, 054013 (2021).
[4] P. Bargiela, F. Caola, A. von Manteuffel, and L. Tancredi, Three-loop helicity amplitudes for diphoton production in gluon fusion, J. High Energy Phys. 02 (2022) 153.
[5] F. Caola, A. Chakraborty, G. Gambuti, A. von Manteuffel, and L. Tancredi, Three-Loop Gluon Scattering in QCD and the Gluon Regge Trajectory, Phys. Rev. Lett. **128**, 212001 (2022).
[6] F. Caola, A. Chakraborty, G. Gambuti, A. von Manteuffel, and L. Tancredi, Three-loop helicity amplitudes for four-quark scattering in massless QCD, J. High Energy Phys. 10 (2021) 206.
[7] F. Caola, A. Chakraborty, G. Gambuti, A. von Manteuffel, and L. Tancredi, Three-loop helicity amplitudes for quark-gluon scattering in QCD, J. High Energy Phys. 12 (2022) 082.
[8] J. M. Campbell, R. K. Ellis, and C. Williams, Direct Photon Production at Next-to–Next-to-Leading Order, Phys. Rev. Lett. **118**, 222001 (2017); **124**, 259901(E) (2020).
[9] T. Peraro and L. Tancredi, Physical projectors for multi-leg helicity amplitudes, J. High Energy Phys. 07 (2019) 114.
[10] T. Peraro and L. Tancredi, Tensor decomposition for bosonic and fermionic scattering amplitudes, Phys. Rev. D **103**, 054042 (2021).
[11] L. J. Dixon, Calculating scattering amplitudes efficiently, arXiv:hep-ph/9601359.
[12] F. Cascioli, P. Maierhofer, and S. Pozzorini, Scattering Amplitudes with Open Loops, Phys. Rev. Lett. **108**, 111601 (2012).
[13] F. Buccioni, J.-N. Lang, J. M. Lindert, P. Maierhöfer, S. Pozzorini, H. Zhang, and M. F. Zoller, OpenLoops 2, Eur. Phys. J. C **79**, 866 (2019).
[14] C. Anastasiou, E. W. N. Glover, and M. Tejeda-Yeomans, Two loop QED and QCD corrections to massless fermion boson scattering, Nucl. Phys. **B629**, 255 (2002).
[15] S. Catani, The singular behavior of QCD amplitudes at two loop order, Phys. Lett. B **427**, 161 (1998).
[16] P. Nogueira, Automatic Feynman graph generation, J. Comput. Phys. **105**, 279 (1993).
[17] J. Vermaseren, New features of FORM, arXiv:math-ph/0010025.
[18] K. Chetyrkin and F. Tkachov, Integration by parts: The algorithm to calculate beta functions in 4 loops, Nucl. Phys. **B192**, 159 (1981).
[19] S. Laporta, High precision calculation of multiloop Feynman integrals by difference equations, Int. J. Mod. Phys. A **15**, 5087 (2000).
[20] C. Studerus, Reduze-Feynman integral reduction in C++, Comput. Phys. Commun. **181**, 1293 (2010).
[21] A. von Manteuffel and C. Studerus, Reduze 2—Distributed Feynman integral reduction, arXiv:1201.4330.
[22] A. von Manteuffel and R. M. Schabinger, A novel approach to integration by parts reduction, Phys. Lett. B **744**, 101 (2015).
[23] J. Gluza, K. Kajda, and D. A. Kosower, Towards a basis for planar two-loop integrals, Phys. Rev. D **83**, 045012 (2011).

[24] H. Ita, Two-loop integrand decomposition into master integrals and surface terms, Phys. Rev. D **94**, 116015 (2016).
[25] K. J. Larsen and Y. Zhang, Integration-by-parts reductions from unitarity cuts and algebraic geometry, Phys. Rev. D **93**, 041701 (2016).
[26] J. Böhm, A. Georgoudis, K. J. Larsen, M. Schulze, and Y. Zhang, Complete sets of logarithmic vector fields for integration-by-parts identities of Feynman integrals, Phys. Rev. D **98**, 025023 (2018).
[27] R. M. Schabinger, A new algorithm for the generation of unitarity-compatible integration by parts relations, J. High Energy Phys. 01 (2012) 077.
[28] B. Agarwal, S. P. Jones, and A. von Manteuffel, Two-loop helicity amplitudes for $gg \to ZZ$ with full top-quark mass effects, J. High Energy Phys. 05 (2021) 256.
[29] A. von Manteuffel and R. M. Schabinger, Quark and gluon form factors to four-loop order in QCD: The N_f^3 contributions, Phys. Rev. D **95**, 034030 (2017).
[30] T. Peraro, Scattering amplitudes over finite fields and multivariate functional reconstruction, J. High Energy Phys. 12 (2016) 030.
[31] T. Peraro, FiniteFlow: Multivariate functional reconstruction using finite fields and dataflow graphs, J. High Energy Phys. 07 (2019) 031.
[32] E. Remiddi and J. Vermaseren, Harmonic polylogarithms, Int. J. Mod. Phys. A **15**, 725 (2000).
[33] J. Henn, B. Mistlberger, V. A. Smirnov, and P. Wasser, Constructing d-log integrands and computing master integrals for three-loop four-particle scattering, J. High Energy Phys. 04 (2020) 167.
[34] J. M. Henn, Multiloop Integrals in Dimensional Regularization Made Simple, Phys. Rev. Lett. **110**, 251601 (2013).
[35] See Supplemental Material at http://link.aps.org/supplemental/10.1103/PhysRevD.107.L051502 for constants definitions and analytic results of scattering amplitudes.
[36] G. F. Sterman and M. E. Tejeda-Yeomans, Multiloop amplitudes and resummation, Phys. Lett. B **552**, 48 (2003).
[37] S. Mert Aybat, L. J. Dixon, and G. F. Sterman, The Two-Loop Anomalous Dimension Matrix for Soft Gluon Exchange, Phys. Rev. Lett. **97**, 072001 (2006).
[38] S. Mert Aybat, L. J. Dixon, and G. F. Sterman, The two-loop soft anomalous dimension matrix and resummation at next-to-next-to leading pole, Phys. Rev. D **74**, 074004 (2006).
[39] T. Becher and M. Neubert, Infrared Singularities of Scattering Amplitudes in Perturbative QCD, Phys. Rev. Lett. **102**, 162001 (2009); **111**, 199905(E) (2013).
[40] T. Becher and M. Neubert, On the structure of infrared singularities of gauge-theory amplitudes, J. High Energy Phys. 06 (2009) 081; 11 (2013) 024(E).
[41] L. J. Dixon, Matter Dependence of the three-loop soft anomalous dimension matrix, Phys. Rev. D **79**, 091501 (2009).
[42] E. Gardi and L. Magnea, Factorization constraints for soft anomalous dimensions in QCD scattering amplitudes, J. High Energy Phys. 03 (2009) 079.
[43] E. Gardi and L. Magnea, Infrared singularities in QCD amplitudes, Nuovo Cimento Soc. Ital. Fis. **32N5-6**, 137 (2009).
[44] O. Almelid, C. Duhr, and E. Gardi, Three-Loop Corrections to the Soft Anomalous Dimension in Multileg Scattering, Phys. Rev. Lett. **117**, 172002 (2016).
[45] G. P. Korchemsky and A. V. Radyushkin, Renormalization of the Wilson loops beyond the leading order, Nucl. Phys. **B283**, 342 (1987).
[46] S. Moch, J. A. M. Vermaseren, and A. Vogt, The three loop splitting functions in QCD: The nonsinglet case, Nucl. Phys. **B688**, 101 (2004).
[47] J. Blümlein, P. Marquard, C. Schneider, and K. Schönwald, The three-loop unpolarized and polarized non-singlet anomalous dimensions from off shell operator matrix elements, Nucl. Phys. **B971**, 115542 (2021).
[48] A. Vogt, S. Moch, and J. A. M. Vermaseren, The three-loop splitting functions in QCD: The singlet case, Nucl. Phys. **B691**, 129 (2004).
[49] A. Grozin, J. M. Henn, G. P. Korchemsky, and P. Marquard, Three Loop Cusp Anomalous Dimension in QCD, Phys. Rev. Lett. **114**, 062006 (2015).
[50] J. M. Henn, G. P. Korchemsky, and B. Mistlberger, The full four-loop cusp anomalous dimension in $\mathcal{N} = 4$ super Yang-Mills and QCD, J. High Energy Phys. 04 (2020) 018.
[51] T. Huber, A. von Manteuffel, E. Panzer, R. M. Schabinger, and G. Yang, The four-loop cusp anomalous dimension from the $N = 4$ Sudakov form factor, Phys. Lett. B **807**, 135543 (2020).
[52] A. von Manteuffel, E. Panzer, and R. M. Schabinger, Cusp and Collinear Anomalous Dimensions in Four-Loop QCD from Form Factors, Phys. Rev. Lett. **124**, 162001 (2020).
[53] V. Ravindran, J. Smith, and W. L. van Neerven, Two-loop corrections to Higgs boson production, Nucl. Phys. **B704**, 332 (2005).
[54] S. Moch, J. A. M. Vermaseren, and A. Vogt, The quark form-factor at higher orders, J. High Energy Phys. 08 (2005) 049.
[55] S. Moch, J. Vermaseren, and A. Vogt, Three-loop results for quark and gluon form-factors, Phys. Lett. B **625**, 245 (2005).
[56] B. Agarwal, A. von Manteuffel, E. Panzer, and R. M. Schabinger, Four-loop collinear anomalous dimensions in QCD and $N = 4$ super Yang-Mills, Phys. Lett. B **820**, 136503 (2021).
[57] C. Duhr and F. Dulat, PolyLogTools—Polylogs for the masses, J. High Energy Phys. 08 (2019) 135.